

# Estimating Channel Storage and Discharge Hydrographs of Flooding

Shoji FUKUOKA<sup>1</sup>, Akihide WATANABE<sup>2</sup>

To estimate channel storage and reduction of peak discharge—unique properties of flood flows—the authors performed intense, fully planned observation of flooding in a 7-km section of the Edo River and carried out a detailed investigation of the longitudinal distribution of discharge and water level hydrographs. Then, the water level hydrographs by this temporally and spatially intense observation were used to estimate storage and discharge hydrographs of the observed flood flow in accordance with a two-dimensional unsteady flow analysis technique developed by the authors. The accuracy of flood flow observation was examined through intense observation and analysis and recommendations are made for a method of flood observation that should prove useful in estimating channel storage and reduction in peak discharge.

## 1. Introduction

In a compound channel, discharge decreases in the rising-water phase, as floodwaters flow into the flood channel, and increases in the receding-water phase, as floodwaters flow back into the main channel from the flood channel. Consequently, discharge in a compound channel during flooding varies longitudinally with distance downstream, such that peak discharge decreases with distance downstream. Laboratory studies have shown that peak discharge decreases particularly when the main channel meanders or the flood channel has a high roughness coefficient<sup>1), 2), 3)</sup>. Field observation<sup>3)</sup> and numerical analysis<sup>4)</sup> of flood hydrograph transformation and channel storage in actual rivers is being carried out to arrive at a method for estimating longitudinal changes in the discharge hydrograph and reduction in peak discharge in such compound channels because such a method would be highly significant with regard to river planning and flood safety assessment. This paper discusses the analysis of temporal and spatial changes in water surface profile and discharge of flood flow as determined by intense observation in a 7-km section of the Edo River (between the 39 km and 46 km points) and presents a method for estimating the discharge hydrograph from Observed flood level hydrographs for the Edo River and a two dimensional unsteady flow analysis. Then, the accuracy of intense observation is discussed, and a method for flood observation is proposed.

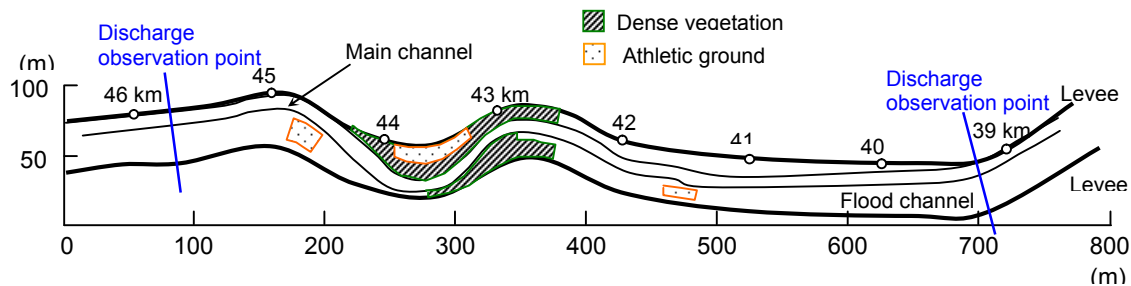


Fig.1 Planform of the Edo River section observed (46.0km – 39.0km)

<sup>1</sup> Professor, Department of Social and Environmental Engineering, Graduate School of Engineering, Hiroshima University, Japan, ph.+81-824-24-7821, fax +81-824-24-7821, [sfuku@hiroshima-u.ac.jp](mailto:sfuku@hiroshima-u.ac.jp)

<sup>2</sup> Associate Professor, Department of Social and Environmental Engineering, Graduate School of Engineering, Hiroshima University, Japan, ph.+81-824-24-7819, fax +81-824-24-7821, [awata@hiroshima-u.ac.jp](mailto:awata@hiroshima-u.ac.jp)

## 2. Analysis of Channel Storage and Reduction in Peak Discharge

Figure 1 shows the planform and ground cover condition of the Edo River section observed. The flood channel of this section, located between upstream and downstream discharge observation sections, is primarily grassland, with other, more substantive vegetation distributed sparsely over a large area. Vegetation growth is dense between the 42.5 km and 44 km points. Some parts of the flood channel are used as athletic grounds, and a golf course exists on the right bank, on a site whose upstream boundary is near the 41 km point. In the analysis, velocity was calculated using the following equations of motion in the general coordinate system:

$$\begin{aligned} & \frac{\partial \tilde{U}}{\partial t} h + \tilde{U} h \left\{ \frac{\partial \tilde{U}}{\partial \tilde{\xi}} - \tilde{J} (\tilde{V} - \tilde{U} \cos \theta^{\eta\xi}) \frac{\partial \theta^{\xi}}{\partial \tilde{\xi}} \right\} + \tilde{V} h \left\{ \frac{\partial \tilde{U}}{\partial \tilde{\eta}} - \tilde{J} (\tilde{V} - \tilde{U} \cos \theta^{\eta\xi}) \frac{\partial \theta^{\xi}}{\partial \tilde{\eta}} \right\} = -gh \left\{ \frac{\partial \zeta}{\partial \tilde{\xi}} + \cos \theta^{\eta\xi} \frac{\partial \zeta}{\partial \tilde{\eta}} \right\} - \tau_{z\xi} \\ & + \frac{1}{J} \left[ \frac{\partial}{\partial \tilde{\xi}} \left( \frac{Jh}{d\xi} \tilde{\tau}_{\xi\xi} \right) + \frac{\partial}{\partial \tilde{\eta}} \left( \frac{Jh}{d\eta} \tilde{\tau}_{\xi\eta} \right) \right] - \tilde{J} h (-\tilde{\tau}_{\xi\xi} \cos \theta^{\eta\xi} + \tilde{\tau}_{\xi\eta}) \frac{\partial \theta^{\xi}}{\partial \tilde{\xi}} - \tilde{J} h (-\tilde{\tau}_{\xi\eta} \cos \theta^{\eta\xi} + \tilde{\tau}_{\eta\eta}) \frac{\partial \theta^{\xi}}{\partial \tilde{\eta}} \end{aligned} \quad (1)$$

where the shear stress term  $\tau_{z\xi}$  represents bottom shear stress and the fluid resistance resulting from the vegetation. This is determined as follows using the Manning roughness coefficient  $n$  and the vegetation permeability coefficient  $K$ , revealing the difference in resistance variance according to depth:

$$\tau_{z\xi} = \left( \frac{gn^2}{h^{1/3}} + \frac{gh}{K^2} \right) \sqrt{u^2 + v^2} \tilde{U}, \quad u^2 + v^2 = \tilde{J}^2 (\tilde{U}^2 - 2\tilde{U}\tilde{V} \cos \theta^{\eta\xi} + \tilde{V}^2) \quad (2)$$

Table 1 Coefficients of Manning roughness and vegetation permeability

Place		Roughness coefficient	Place		Vegetation permeability coefficient (m/sec)
Main channel		0.029			
Flood channel ground		0.031	46.0-43.5 km	Right bank	60.0
46.0-43.0 km	Right bank	0.044	43.5-42.5 km		30.0
	Left bank	0.038	42.5-42.0 km		40.0
43.0-42.0 km	Right bank	0.049	42.0-40.5 km	Left bank	60.0
	Left bank	0.049	44.5-43.0 km		45.0
42.0-40.5 km	Right bank	0.044	43.0-42.0 km		50.0
	Left bank	0.044	42.0-41.0 km	60.0	
40.5-39.0 km	Right bank	0.038			
	Left bank	0.038			

The Manning coefficients for main channel and flood channel roughness and vegetation permeability used in the analysis were determined so that the calculated discharges and surface profiles would generally match the observed values; these assumed values are listed in Table 1. Because the vegetation could not be precisely positioned in the calculation mesh, an average vegetation permeability coefficient for the entire flood channel was used with the roughness coefficient. Figure 2 shows the cross-sectional shape of the 39–46 km section used in the analysis. In this section, the main channel is 80–120 m wide; the distance between levees, roughly 400 m. Flooding was observed over a 48-hour time period lasting from 12:00 a.m. September 11 to 12:00 a.m. September 13. Thus, the start time in the calculations is also 12:00 a.m. on the 11th.

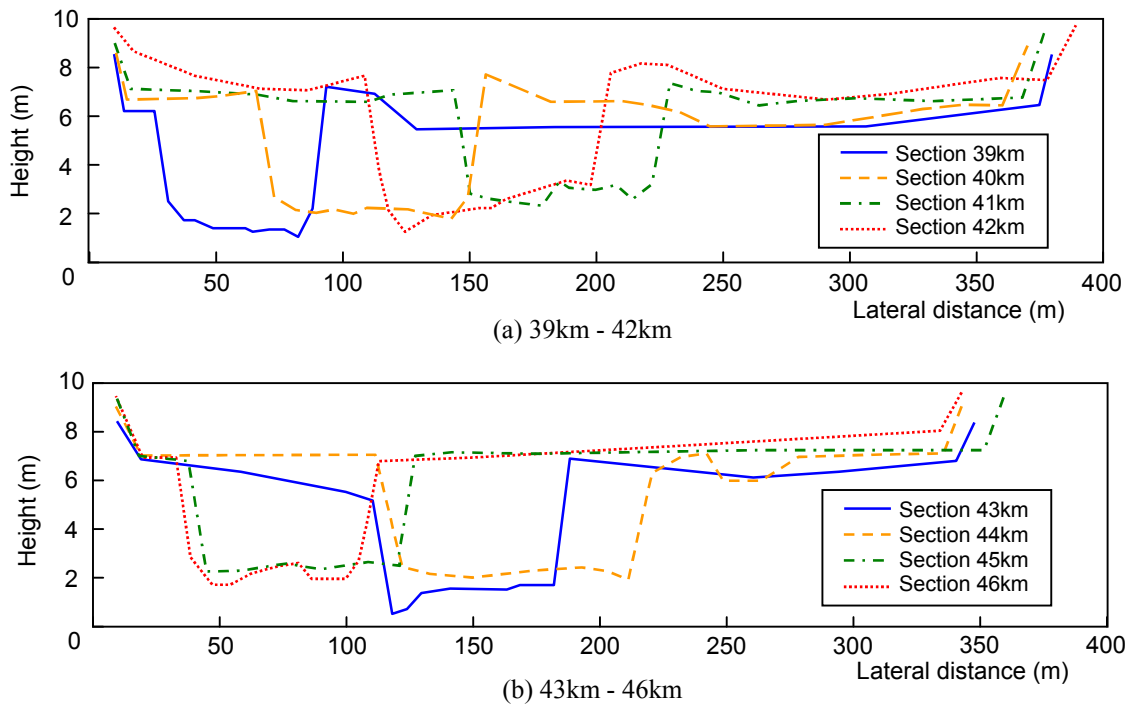


Fig. 2 Cross-sectional shape (39km - 46km)

In ordinary unsteady flow analysis, discharge at the upstream end and water level at the downstream end is given, and temporal change in discharge and water level is calculated. During observation of Edo River flooding on September 11, discharge at the upstream and downstream ends was observed nearly every hour. Water level was observed on the left and right banks roughly each hour at intervals of 0.25 km in the 46–41 km section and at 0.5 km intervals in the 41–39 km section. However, as discussed below, the values for upstream and downstream end discharge observed each hour contained error that resulted in a large difference in discharges, thus failing to satisfy the continuity conditions.

In general, error in observed discharge is considered to be greater than error in the profile of water level observed at multiple points. In the authors' analysis, because observed water level is assumed to have the greater accuracy, water level at the upstream and downstream ends is given, and roughness is adjusted so that the calculated discharge for the upstream end matches the corresponding observed discharge.

Figure 3 is a flowchart of the overall analysis procedure. As it shows, the first step is to create the boundary conditions from the observed values by interpolating time series data for upstream and downstream end water level. In this stage, one cycle of flood calculations is performed while measuring error and adjusting upstream and downstream water levels as in a model experiment so as to eliminate error, so that calculated water level for each specified location at each time point agrees with the observed values. Next, the calculated discharge hydrograph and calculated temporal variation in the longitudinal distribution of water level are compared with the observed results, after which the absolute value and relative distribution of the coefficients of roughness and vegetation permeability are altered so as to bring the observed and calculated results closer to agreement. Flood flow calculations are repeated until the calculations obtained match the observed results. Because discrepancy between the calculations and the observed results can also result from poor accuracy in the observations, care is required to determine whether such discrepancy is due to unadjusted data or to observation error.

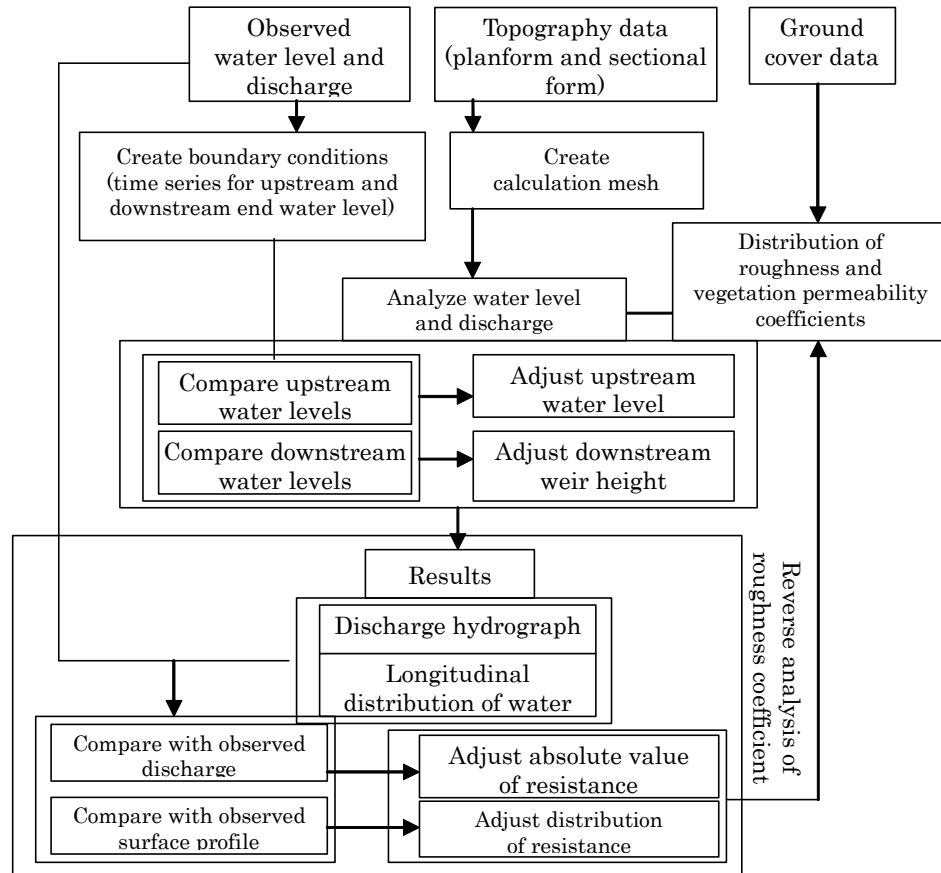


Fig 3 Flowchart of overall analysis.

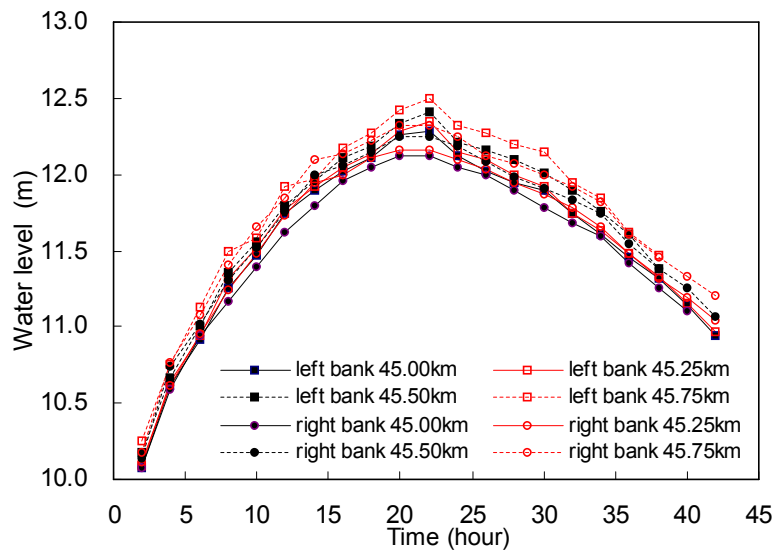


Fig.4 Temporal change in observed water level in an upstream part

Figure 4 shows temporal changes in observed water level in an upstream part (45–45.75 km) of the observed section. The considerable variation in observed water level at the left and right banks in this upstream section is believed to reflect considerable observation error. With the calculation mesh positioned so that the right bank water level at the 45 km point corresponds to the right bank at the mesh's 45 km point, water level at the downstream end discharge observation point was used as the average downstream end water level for the

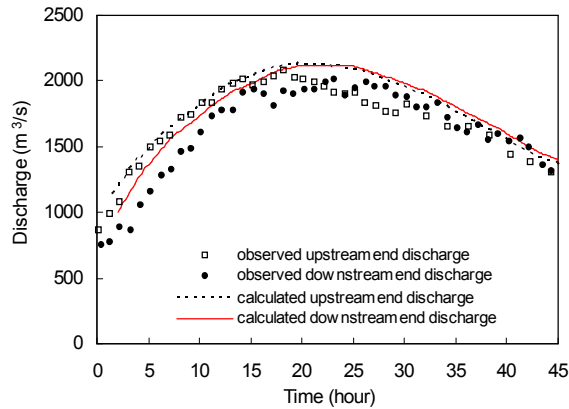


Fig.5 Comparison between the observed and calculated discharge

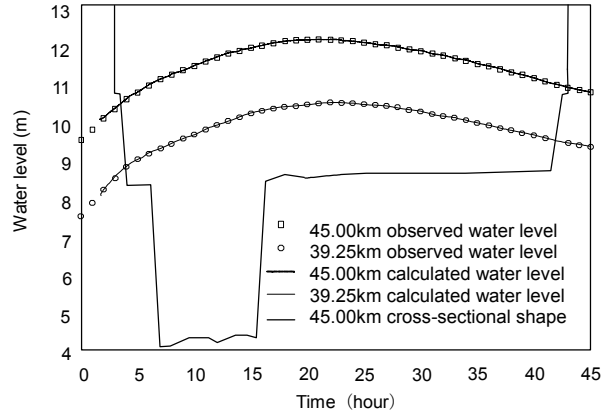


Fig.6 Observed and calculated water levels for the upstream and downstream ends and cross-sectional shape at the 45km point

calculation mesh. In the calculations, water levels at the upstream and downstream ponds in the mesh are automatically adjusted so that the observed and calculated water levels for these sections agree<sup>3)</sup>.

Figure 5 shows the calculated and observed discharges for the upstream and downstream end discharge observation points. Figure 6 shows the observed and calculated water levels for the 45 km point (upstream) and the downstream end discharge observation point, along with the channel's cross-sectional shape at the 45 km point. The figures show that the upstream and downstream water levels roughly satisfy the given boundary conditions. At 12:00 a.m. on the 11th (the analysis start time), water level at the 45 km point is 9.5 m, with roughly 1 m of water in the flood channel. The observed section's flood channel also exhibits the same amount of water levels. As for discharge, because the analysis is synchronized to the discharge at the upstream end in the rising-water phase, calculated upstream discharges in the rising-water phase agree well with observed discharges. However, calculated discharges at the downstream end are larger than the observed values. Comparison of calculated and observed discharges shows that at the time of peak water level, observed discharge upstream has already dropped considerably even though water level has continued to rise. Such a state is inconceivable in light of the continuity relationship of water level. On the other hand, the upstream and downstream end discharges in the receding-water phase present no problem within the range of observation accuracy. Although further investigation is needed, it is believed that there was some problem with discharge observation accuracy at the upstream end in the rising-water phase. Ordinarily, there should be almost no difference between peak discharges upstream and downstream, and the difference between calculated discharge and observed upstream end discharge at the peak should be almost the same as that during the receding-water phase. However, this difference is more than 100m<sup>3</sup>/s, suggesting that observed discharge during the rising-water phase was probably overestimated.

### 3. Results of Analysis and Consideration

As Figure 5 shows, calculated discharge changes slightly with distance downstream, but peak discharge hardly decreases at all. Peak discharge falls less than 0.5% ( $10 \text{ [m}^3/\text{s}]/2100 \text{ [m}^3/\text{s}]$ ) roughly 6.5 km downstream from its occurrence. Because temporal change in discharge in the Edo River is very gradual, peak discharge and water level both continued for 3–4 hours in the observed section, as shown in Figures 5 and 6. Considering that the flood travel time in the observed section is 1–2 hours, discharge and water level remained nearly

constant at and around the peak. This is believed to explain the low amount of storage associated with the flood flow's unsteadiness. Similar results for storage can be expected so long as agreement with observed water level profiles is sought in water surface profile analysis, regardless of what values are used for the discharge or roughness coefficients. For this section to have an unsteady flow characteristics and thus make considerable channel storage of the floodwaters possible would require the type of flood hydrograph that precludes steady flows, i.e., a time scale that is one-third to one-fourth of this particular flood's time scale. Flood hydrographs in the Maruyama River do have a time scale that is conducive to such unsteady flows<sup>4)</sup>, and this is believed to explain the significant decrease in discharge that occurs there. Figure 7 shows the longitudinal distribution of observed and calculated water level in the rising-water phase (7a), at peak water level (7b), and in the receding-water phase (7c). Excepting the 43 km point, the calculated values generally agree with the observed values. Although the water level increase near the 43 km point is attributable to vegetation, increasing the resistance of the vegetation in the calculations does not yield as great an increase as was observed there; in fact, only a local rise in surface slope occurs, such that overall agreement in surface profile is lost. In addition, 22 hours after the start of flooding (i.e., at peak), observed water level on the left bank of the 46–43 km section was 20 cm higher than the calculated water level and the observed water level on the right bank. However, because it

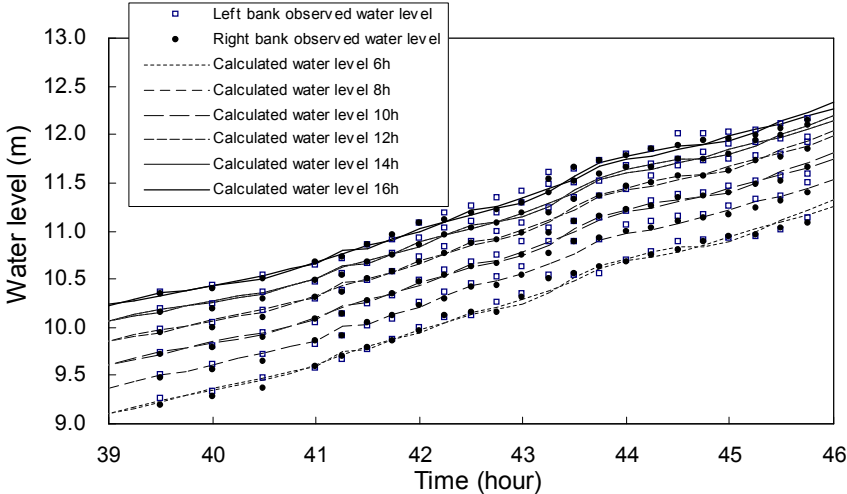


Fig.7(a) Longitudinal distribution of observed and calculated water level (rising-water phase)

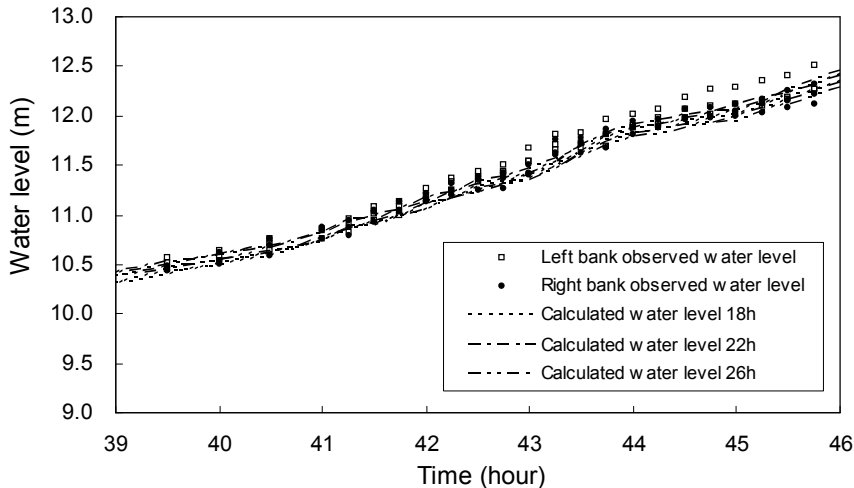


Fig.7(b) Longitudinal distribution of observed and calculated water level (peak-water level phase)

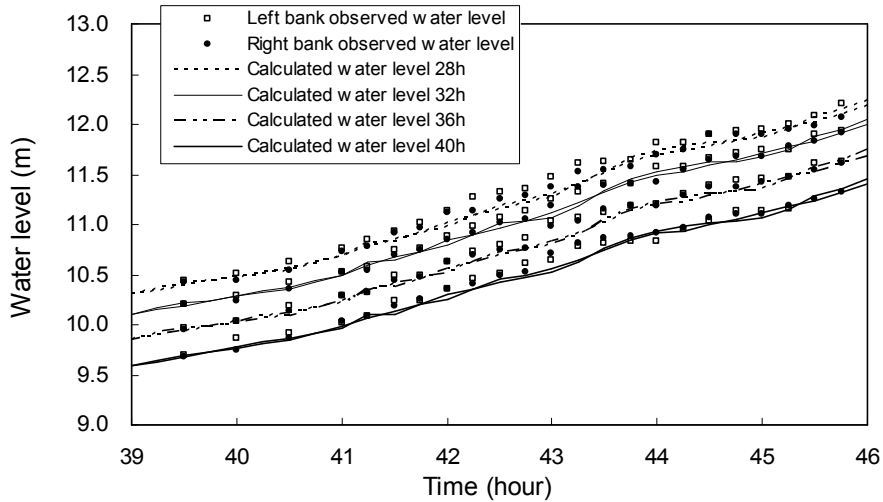


Fig.7(c) Longitudinal distribution of observed and calculated water level (receding-water phase)

is inconceivable that the left bank water level could be higher at the peak—when discharge is roughly constant—this is likely a result of observation error. The preceding shows that temporal change in surface profile can be easily tracked using numerical methods.

In the 45.75–39.5 km section, cross-section-averaged water levels were calculated for observed and calculated values by averaging the left and right bank water levels; these averages, weighted by each section's water surface area, are shown in Figure 8. (Note that the data are presented in 2-hour increments.) Multiplying a section's surface area by the change in water level in Figure 8 produces the amount of storage, which is time-differentiated to yield the storage per unit time. The temporal change each 2 hours in mean storage rate in the section as calculated from the values in Figure 8 is shown in Figure 9, along with the difference between calculated and observed values for upstream and downstream discharge.

Figure 8 shows that the calculations can reproduce floodwater storage in the observed section. The differences at peak in Figure 8 are, as already shown in Figure 4, due to the higher observed water level upstream on the left bank at peak. The agreement, seen in Figure 9, between the storage rate ( $dS/dt$ ) determined from observed and calculated water surface profile and the storage rate determined from the calculated discharge differential ( $Q_{in}-Q_{out}$ )

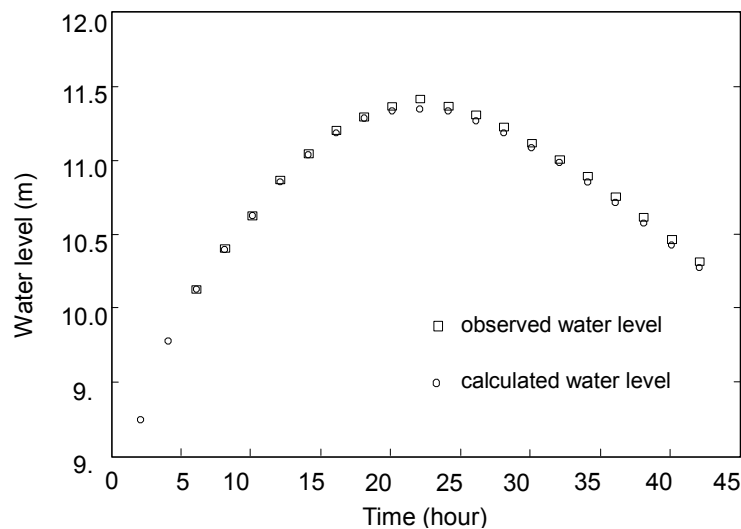


Fig.8 Temporal change in average water level in the observed section

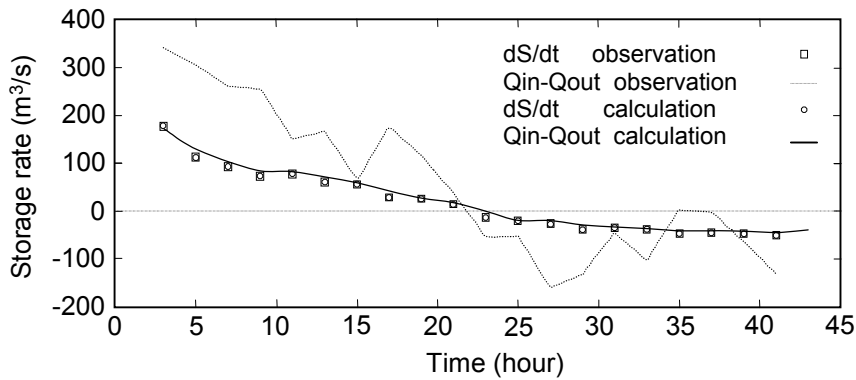


Fig.9 Temporal change in storage rate

indicates the numerical method's high reproducibility with regard to actual floodwater storage. The storage rates are low:  $100 \text{ m}^3/\text{s}$  in the rising-water phase and  $-40 \text{ m}^3/\text{s}$  in the receding-water phase. These low storage rates, along with the small difference in shapes between the rising- and receding-water phases, indicate that extensive storage did not occur and that discharge hydrograph transformation was consequently low in this flood. On the other hand, the storage rate determined from observed discharge exceeds the actual storage rate in the rising-water phase but is less than the actual storage rate in the receding-water phase.

Because the reduction in discharge over a section of several kilometers is on the order of at most several percentage points relative to peak discharge, discharge must be measured correctly to be accurate at a percentage level. However, as the results of these calculations show, if the accuracy of field observation is to be taken into account, then the quantitative reduction in peak discharge can be determined more accurately with a method that tracks temporal change in profile than it can be with observed discharge. In other words, the detailed observation of water levels is the superior method for assessing channel storage in actual rivers.

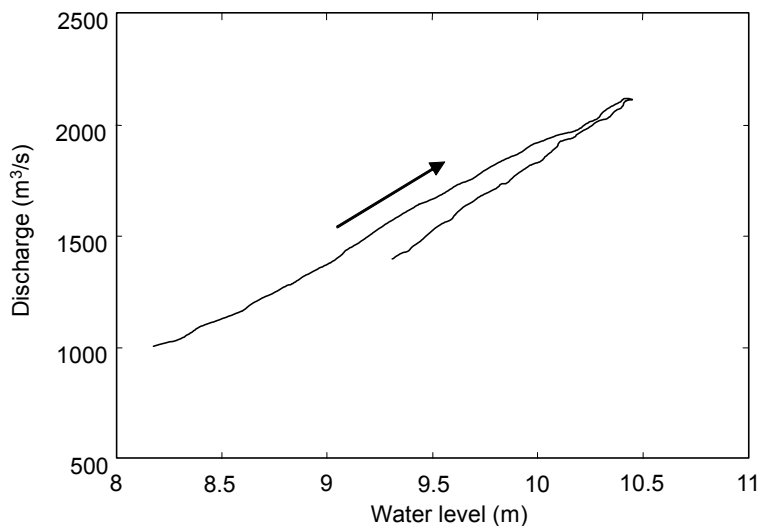


Fig.10 Calculated water level and discharge relationship for the downstream end discharge observation point (39.25km)

The calculated water level–discharge curve for the downstream end discharge observation point (Figure 10) is a clockwise-looping curve. However, the loop is extremely narrow, almost overlapping at the peak, indicating particular small unsteadiness near the peak. Because the degree of unsteadiness depends on the relationship between flood travel time (itself determined by flood flow velocity and section length) and the duration of the steady



phase at peak, either the time scale of the flood hydrograph is shortened, yielding a sharp discharge hydrograph, or a longer observed section is chosen to increase the effect of unsteadiness, i.e., to manifest the effect of the channel storage of floodwaters.

The Edo River flood considered in this paper had poor unsteadiness, particularly near the peak, so that there is almost no decrease in discharge with distance downstream. In addition, variation in channel storage and peak discharge can be estimated by adjusting the calculated surface profile at each point in time to the observed surface profile. Accurate estimations of a discharge hydrograph require accurate values for observed discharge, but the temporal change in discharge between its low and high values can be back-calculated with measurements from only several points therebetween; such a technique should be especially useful for estimating peak discharge. The accuracy of discharge estimated by this technique is directly determined by the accuracy of observed discharge. Observed discharge used by the authors contained error on the order of  $100 \text{ m}^3/\text{s}$  because of the relatively short section at whose upstream and downstream ends discharge was measured and because of detailed measurements of surface profile. The authors were able to assess this error quantitatively by observing upstream and downstream discharge and by tracking surface profile. An error of  $100 \text{ m}^3/\text{s}$  corresponds to merely 5% of peak discharge in the Edo River. The degree of error depends on the accuracy of the discharge observation technique, and although accuracy is difficult to improve, the observation technique used by the authors in the Edo River makes it possible to determine the degree of error in observed discharge. For a slow-moving flood such as the one considered herein, an effective means of determining the transformation of a discharge hydrograph over a long distance is to define a long section (i.e., one on the order of tens of kilometers long), establish therein multiple sections for the intense observation of discharge and water level, use the observed results to validate calculated discharge, and track the temporal change in surface profile over a long range using observation point water level and other data.

Discharge hydrograph transformation and peak discharge reduction have been shown to occur in cases where discharge changes over a short time scale as in the Maruyama River study, in which the observation section length (5 km), river width (250 m), discharge, and water level change were similar<sup>4</sup>). The time required for peak discharge to decrease 50% was significantly longer in the Edo River (peak discharge  $2,100 \text{ m}^3/\text{s}$ ) than in the Maruyama River (peak discharge  $2,500 \text{ m}^3/\text{s}$ ): 10 times longer in the rising-water phase and 6–7 times longer in the receding-water phase. The Edo River's hydrograph overall is a U-shaped curve, whereas that of the Maruyama river is an inverted U-shaped curve in the receding water phase because of the sharply dropping discharge. Flood flow unsteadiness affects hydrograph shape and time scale and has a great effect on the tendency of peak discharge to decrease with distance downstream. However, even when discharge changes this abruptly, tracking of temporal change in surface profile makes it possible to estimate peak discharge (from surface form) and changes in peak discharge without the need for intense observation of discharge.

Although automation of discharge observation is still difficult in view of current technology and accuracy considerations, automated water level and surface profile observation is possible. Therefore, it should be possible to estimate temporal change in discharge accurately and with less labor-intensive discharge observation by using a method in which temporal change in discharge is estimated by numerical analysis and by the tracking of temporal change in surface profile, with the data necessary for computational calibration provided by a small number of discharge observation points. However, as already stated, the accuracy of discharge values depends on the accuracy of discharge observation.

Furthermore, in both the Edo and Maruyama River studies, observation began after waters had already started to flow into the flood channel, but because the channel storage rate increases greatly when water enters the flood channel, measurements for the longitudinal

distribution of water level should, at the very least, begin before this point. When surface profile has been tracked, discharge and roughness calibration can be performed to generate a discharge hydrograph for that period. In this respect, too, it is hoped that water level observation will be automated to the degree that longitudinal change in surface profile can be determined.

#### **4. Issues for Future Consideration**

Channel storage of a flood flow and the decrease in peak discharge vary depending on the observed section's flood hydrograph properties (e.g., unsteadiness and peak discharge) and on channel properties (e.g., planform, cross-sectional form, and flood channel roughness). For the Edo River, the relationship between the temporospatial distribution of rainfall in the draining basin and the hydrographs of previous floods should be thoroughly investigated to determine what type of flood hydrographs should be anticipated in the flood control planning. Further, now that this research has essentially established a practical method for the unsteady flow analysis of flood flows, the next step is to assess this method's accuracy by calculating the downstream transformation of discharge hydrographs and storage through two-dimensional unsteady flow analysis using the water level hydrographs from all automatic water level observation points in a long river section and using discharge data on channel cross-sectional form and planform taken at 200-m intervals. The next task is to thus establish a method for assessing storage and peak discharge reduction in river sections and to appropriately incorporate such storage rate quantities into planning throughout a river extension.

#### **References**

- (1)Shoji Fukuoka, Akihide Watanabe, Hirokazu Okabe and Koh-tarou Seki (2000) : Effects of Unsteadiness, Planform and Cross-Sectional Form of Channels on Hydraulic Characteristics of Flood Flow, Annual Journal of Hydraulic Engineering, JSCE, Vol.44.pp.867-872.
- (2) Shoji Fukuoka, Koh-tarou Seki and Daisuke Kurisu (2000) : Flood Flow Storage and Peak Discharge Attenuation in Channels, Advances in River Engineering, Vol.6, pp.31-36.
- (3)Akihide Watanabe, Shoji Fukuoka, Alex George Mutasingwa and Masaru Ota (2002) : The Unsteady 2D Flow Analysis on the Deformation of Hydro-Graph and the Flood Flow Storage in Compound Meandering Channels, Annual Journal of Hydraulic Engineering, JSCE, Vol.46.pp.427-432.
- (4)Shoji Fukuoka, Daisuke Kurisu, Alex George Mutasingwa, Tsuyoshi Nakamura and Masanori Takahashi (2002) : Effect of Levee and Main Channel Alignments and Flood Channel Width on Water Storage During Flood Flow, Annual Journal of Hydraulic Engineering, JSCE, Vol.46.pp.433-438.